

Models for Flow Efficiency Assessment in Oil and Gas Pipelines

Njoki E. Marigi^{1*}, Jiping Bai¹, Kinuthia M. John¹, Paul Davies¹, Ngila J. Catherine²

¹*Faculty of Computing, Engineering, and Science, University of South Wales, Pontypridd CF37*

1DL, United Kingdom, +44 345 576 0101

²*Department of Chemical Sciences University of Johannesburg, P.O. Box 17011,*

Doornfontein

Johannesburg 2028, South Africa

**Corresponding Author*

Abstract

Flow efficiency is largely affected by deposits and corrosion in pipelines. The purpose of this study was to develop models for assessing the effect of deposits and corrosion on flow efficiency in oil and gas pipelines to ensure production and safety. A new advanced analytical method developed in this study was employed. The data required involved in-line inspection data and Supervisory Control and Data Acquisition obtained from the test pipeline. Samples used for the study involved the test and control pipeline laid parallel to each other. The resulting models were capable of predicting the flow efficiency as well as assessing the effects of deposits and corrosion with high accuracy indicated by an error of 3% when compared with similar field values. To reduce the effects of deposits and corrosion on flow efficiency, an optimal pigging frequency model was developed with results agreeing well with those from the existing literature.

Keywords: Flow efficiency mathematical Models; Influence factors; Flow efficiency Chart; Transmission petroleum product pipeline

*Address correspondence to the Faculty of Computing, Engineering and Science, University of South Wales, United Kingdom. Mobile +254 722307676; E-mail: emma.marigi@southwales.ac.uk

1. Introduction

Due to the increase in energy consumption and growing environmental concerns, petroleum-based products hold significant importance in the energy market. In addition to the continuous growth of fuel demand and the development of many remote oil fields, the oil transmission pipelines have not made a rapid improvement as the counterpart gas transmission pipelines. The Global Energy Monitor (Azimi et al., 2020) indicates that the combined length of oil and gas transmission pipelines is presently 2.04 million kilometers. Of this, 1.18 million kilometers is dedicated to gas pipelines, while the remaining 850,000 kilometers is designated for oil pipelines.

Accurate assessment of flow efficiency of oil and gas pipelines is important as it will help operators to know the overall performance and consequently the health condition of the pipeline. A high flow efficiency signifies that the pipe is performing well and vice versa. Karina et al., (2021) confirmed that removal of deposits can help improve flow efficiency both in oil fields and pipelines where they developed a complex technology for removing and preventing the formation of organic deposits. This technology is most applicable for oil field exploration. Other factors known to affect the flow efficiency include length of the pipeline, internal diameter, internal roughness of the pipe, viscosity of the flowing product, density and velocity of the fluid transported in oil and gas pipelines. A knowledge of how these factors affect flow efficiency will help operators prioritize the maintenance activities for the pipelines with respect to the most important factor(s).

Currently, oil and gas pipeline operators anchor their maintenance activities on the 'rule of thumb', alarm alerts and unpredictable catastrophes. According to Wamugo, (2011), this is dangerous as it often results in product loss and leaves behind great damage to the environment and properties and at times loss of lives of people and animals.

During operation, dirt, corrosion products and liquids gather at low lying areas, near 6 o'clock orientation, leading to a decrease of oil flow efficiency. Greater discharge pressure is required for pumps with a lower efficiency, resulting in energy waste and low profitability. Pipeline blockage can lead to fire explosion, pollution, or other ecocatastrophes. To prevent these types of events, oil flow efficiency is adopted to measure the operation situation of oil pipelines for providing technical suggestions on whether pigging should be conducted. Pigging in the oil and gas industry is a form of flow assurance where pipeline pigs are used to purge, clean, and/or inspect pipelines to keep them running smoothly. Due to the operation being hazardous, pigging must only be carried out by experienced personnel. Alternatives for pigging include using corrosion inhibitors such as film former corrosion inhibitors for oil and gas pipelines (Askari et al., 2018). However, these alternatives have the disadvantage of cost as compared with mechanical pigging. Black powder deposits in gas pipelines are effectively removed and controlled by using a combination of both chemical inhibitors and mechanical pigging (Nikolaos and Tsochatzidis, 2007).

Jianbo et al., (2019), reviewed measures used to improve flow efficiency and safety in pipeline operations that include but not limited to accurate prediction of deposition followed by appropriate pigging methods

According to Alamri, (2020), mitigation techniques of localized corrosion are lacking and so mechanical pigging remains the most preferred and economical option.

The oil and gas flow efficiency (E%) is an important parameter showing the working condition and cleanliness of pipelines and can be calculated using ASME B31.4 Code (2002) which estimates flow efficiency as a percentage ratio of actual flow efficiency to design flow efficiency, in Lofti (2015) that estimates flow efficiency using actual flow and maximum flow. Xie (2015) presented a model that estimates gas flow efficiency from theoretical flow and actual flow in the pipeline. Both ASME B31.4 Code (2002) and Lofti (2015) models estimate oil and gas flow efficiencies. All the current methods are limited as they failed to consider the internal condition and factors that affect flow efficiency in oil and gas pipelines. For instance, the Xie (2015) model is limited to gas pipelines only.

Zahid et al. (2018) and Keifner (2001) have discussed the characteristics of multi-product oil and gas pipelines. They are governed by ASME B31.4 code originally established in 1926. The code rules and regulates the transportation in pressure piping systems.

The actual flow rate of pipelines cannot be acquired directly. As the transmission oil and gas pipelines are large in diameter and long in length, the peak shaving ability is large. Peak shaving ability occurs when the oil and gas consumption are in a high peak position and the oil and gas are discharged as a result. The pipeline absolute roughness affects both actual flow rate and estimated flow rate of pipelines and consequently the flow efficiency. A typical multi-product pipeline is shown in Figure 1 with interphases being directed to slop tanks for further processing. Slop tank means a tank specifically designated for the collection of tank draining, tank washings and other oily mixtures or interphases. The aim of this study was to assess flow efficiency, as well as guarantee the safe operation of oil and gas pipelines and associated networks through monitoring the flow efficiency as affected by formation of deposits and corrosion products in transmission pipelines.

2. Methodology

The experimental modelling studies involved investigating a number of factors that influence the flow efficiency and could inform the maintenance activities. The parameters include dimensions of the test pipeline and control pipeline, internal radius of the pipe segment, cross-sectional area, velocity profiles and predicted flow rate, among others.

2.1 Test Pipeline Sample

To simulate the real-life oil and gas pipelines under study, a test pipeline was determined by considering a 1 m length and 350 mm actual diameter of the carbon steel pipe segment for the modelling experiments. Short pipe lengths of 1 m were preferred owing to no friction losses encountered in the pipe segment. Detailed specifications of the test pipeline are shown in Figure 2.

2.2 Control Pipeline Sample

The control pipeline dimensions were 1 m length and 500 mm internal diameter carbon steel control pipe with neither deposits nor corrosion pits as shown in figure 3. The choice of the control pipeline was informed by relatively, newly constructed pipeline in the country which is now four-year-old, for comparison with the old test pipeline which was 43 years old when it was finally abandoned due to flow inefficiency. The studies on flow efficiency of the older pipeline (test pipeline, 1 m length and 350 mm diameter) were compared to those of the control pipeline (relatively new pipeline, 1 m length and 500 mm diameter). In this study, the fact that the test and control pipelines did not have the same dimensions was accounted for by standardization methods. Therefore, the modelling studies considered these shortcomings.

2.3 Determination of the internal and mean radius of the pipe segment

The height or thickness of the deposits from the wall of the pipe is assumed to be axisymmetric about x-axis and vary with x. The height or thickness of the deposits is represented as shown in Equation (1).

$$R_i = R - \varepsilon - t \quad (1)$$

where:

R_i : the reduced radius of the pipeline, mm

ε : the height or thickness of deposits, mm

R : internal radius of the pipeline, mm and

t : the wall thickness, mm

To calculate the flow rate, a mean radius and a mean velocity were used where the mean radial radii were calculated as shown in Equations (2).

$$\begin{aligned} r_1 &= \frac{1}{3} r_m \\ r_2 &= 2r_1 \end{aligned} \quad (2)$$

where:

r_1 : a third of the mean internal radius of the pipe, mm

r_2 : two thirds of the mean internal radius of the pipe, mm

r_m : equal to the mean internal radius of the pipe, mm

The r_m was determined as the mean of the internal radius in a pipeline segment as shown in Equation (3).

$$r_m = \sum_0^n \frac{R_i}{n} \quad (3)$$

where:

r_m : mean of the internal radius in a pipeline segment, mm

n : total number of data points in the pipeline segment

R_i : the reduced radius of the pipeline, mm

2.4 Determination of the Elemental Cross-Sectional Area and Velocity

Figure 4 is a cross - section of a functional multi-product pipeline segment of mean radius r_m and a thickness t , with a radial flow thickness of δr tending to dr , having a perimeter of $2\pi r_m$ or πd_m , where d_m is the mean diameter of flow. Summation of the radial mean area, A_m of flow throughout the pipe cross section is shown in Equation (4).

$$A_m = \pi r_m^2 \tag{4}$$

The product of the mean area of flow and the corresponding mean velocity of flow gives the predicted flow rate throughout the pipeline segment. The **mean velocity** of flow, V_m in the pipeline segment was obtained from velocity profiles drawn by plotting velocities at every third of the radial mean radius of the pipeline segment. These velocities agreed with those obtained analytically using Equation (5) (Peszyrski et al. 2017) for turbulent flow.

$$V_m = 0.8V_{max} \tag{5}$$

where:

V_{max} : maximum velocity of flow throughout the pipeline segment, m/hr.

In turbulent flows through rough pipes, the ratio of the maximum velocity to the mean velocity is dependent on the friction factor. The common **mean velocity distribution** for turbulent flow is given in Equation (6) and (7).

$$\frac{V-V_m}{V^*} = 5.75 \log_{10} \frac{y}{R} + 3.75 \tag{6}$$

where:

V^* : shear velocity, mm/s

V : flow velocity, mm/s

V_m : average velocity, mm/s

y : radial distance across the pipe, mm

R : radius of the pipe, mm

$$V^* = V_m \times \sqrt{\frac{f}{8}} \tag{7}$$

where:

f : friction factor at $y = R$, $V = V_{max}$

$$\frac{V_{max} - V_m}{V_m \times \sqrt{\frac{f}{8}}} = 3.78$$

$$\frac{V_{max}}{V_m} - 1 = \frac{3.78}{\sqrt{8}} \times \sqrt{f}$$

$$\frac{V_{max}}{V_m} = 1 + 1.33 \sqrt{f}$$

$$\frac{V_{max}}{V_m} = 1 + 1.43 \sqrt{f}$$

From Moody chart, $f = 0.01$ for the test pipeline while

$f = 0$ for the control pipeline.

$$\begin{aligned} \therefore \frac{V_{max}}{V_m} &= 1 + 1.43 \\ &= 1.2 \end{aligned}$$

Therefore, the ratio of the maximum velocity to mean velocity is entirely dependent on the friction factor of the pipe which is equivalent to Equation (8).

$$(8) \quad V_m = 0.8 V_{max}$$

where:

$$\begin{aligned} \frac{V_{max}}{V_{mean}} &= \frac{1}{0.8} \\ &= 1.25 \\ &= 1.2 \end{aligned}$$

2.5 Velocity Profiles

Velocity profiles were plotted between radial distances and corresponding velocities. Radial distances were taken as a third of the mean radius of the pipeline segment as shown in Equation (9).

$$\begin{aligned} r_1 &= \frac{1}{3} r_m \\ r_2 &= 2r_1 \end{aligned} \quad (9)$$

where:

r_1 : a third of the mean internal radius of the pipe, mm

r_2 : two thirds of the mean internal radius of the pipe, mm

r_m : equal to the mean internal radius of the pipe, mm

The coefficient of determination, R^2 of the velocity profiles was 95%. The mean velocity, V_m , for mass balance in a turbulent flow in a smooth circular tube with a radius R , at a Reynolds number of about 10^5 is given by Equation (10) Salama (2021).

$$(10) \quad V_m = V_{max} \left(R - \frac{r}{R} \right)^{1/3}$$

where r is the radial distance from the center and V_{max} the maximum velocity at the center. Derive the equation relating to the average velocity (bulk velocity) to V_{max} for an incompressible fluid.

From the velocity profiles, the mean velocity was observed to be about 0.8 of V_{max} as shown in Equation (8).

2.6 Predicted Flow Rate, Q_E

The methodology involved a chart (Figure 5) showing how the predicted flow rate was derived as a product of mean velocity of flow and mean cross-sectional area based on deposits and corrosion in the test pipeline.

The in-line inspection (ILI) data in Figure 5 shows the measured and initial wall thickness (t) of the pipelines. The difference between the wall thickness gave the deposits and corrosion pits in the pipeline. The positive values of the difference in the wall thickness gave deposit height values while the negative values gave the corrosion pit depth values. The cross-sectional area of flow was then determined as shown in the Figure. Velocity of flow was then determined from the ratio of actual flow rates and the cross-section areas just calculated. Velocity of flow just determined was plotted against the radial distances of the pipeline. Maximum velocity of flow was then read off each velocity profile and was then used to determine the mean velocity in turbulent flow as shown in Equation (4). The product of the mean velocity determined, and the mean areas calculated gave the required predicted flow rates in the pipeline. The predicted flow rates and the actual flow rates from the Supervisory Control and Data Acquisition, SCADA were substituted in the flow efficiency mathematical model in Equation (8) to generate the flow efficiency values at any location along the pipeline. The Figure highlights the summary of the method. This is the new advanced analytical method for analyzing turbulent flow in oil and gas pipelines.

2.7 Development of the Flow Efficiency Mathematical Model

Equation (11) shows the developed flow efficiency model for predicting flow efficiency in the oil and gas pipelines. The model is based on predicted and actual SCADA flow rates. SCADA is the current Supervisory Control and Data Acquisition system for monitoring flow efficiency in long distance transmission oil and gas pipelines.

$$E = \left[1 - \frac{\text{abs}(Q_E - Q_{SCADA})}{Q_E} \right] \times 100\% \quad (11)$$

where:

E : the oil and gas flow efficiency, %

Q_{SCADA} : the actual oil flow rate, m^3/hr

Q_E : the estimated or predicted oil and gas flow rate, m^3/hr

The estimated flow rate was predicted using a novel advanced analytical method for turbulent flow in oil and gas pipelines. The actual flows were obtained real time from the Supervisory Control and Data Acquisition, SCADA.

To develop the model, it was assumed that the flow efficiency is a function of predicted flow, Q_E and the actual flow, Q_{SCADA} in the pipeline as shown in Equations (12) – (19).

Therefore:

$$E = f(Q_E) \quad (12)$$

and

$$E = f(Q_{SCADA}) \quad (13)$$

Using the flow rate Equation (14)

$$Q = AV \quad (14)$$

where:

Q : the flow rate, m^3/hr

f : function of

E : the flow efficiency, %

Expressing Q and V as functions of f and g gives:

$$Q = f(A) \quad (15)$$

$$V = g(t)$$

Differentiating (14) and (15) gives Equation (16).

$$\delta q = \frac{\partial q}{\partial v} \delta v \quad (16)$$

Limiting $\delta \rightarrow 0$

$$\frac{dq}{dt} = \frac{\partial q}{\partial v} \frac{dv}{dt} \quad (17)$$

$$Q = Q_0 - \text{Leakage} \quad (18)$$

Assuming:

$$Q_0 = 100\% \text{ (control pipeline) and}$$

$$\text{Leakage} = \left(\frac{Q_E - Q_{SCADA}}{Q_E} \right) \times 100\% \text{ (test pipeline)} \quad (19)$$

where:

Q_0 : Initial flow rate, m^3/hr

Hence, the new developed flow efficiency mathematical model is now derived as shown in Equation (11).

3. Results

3.1 Actual and Predicted Flow Rates in the Test and Control Pipeline

The actual and predicted flow rates in test and control pipelines, were calculated from the Supervisory Control And Data Acquisition (SCADA) system, shown in Table 1.

3.2 Predicted Flow Rates in the Test and Control Pipeline

Continuity equation states that the product of cross-sectional area of the pipe and the fluid velocity at any point along the pipe is always constant. This product is equal to the volume flow per second or simply the flow rate. The continuity equation is given as: $Q = A \times V = \text{constant}$, where Q is the flow rate, A the cross-section area and V is the flow velocity true for laminar flows.

For turbulent flows, where the flow rate is variable, the predicted flow rate was calculated as the integral of product of the mean area of flow and mean velocity of flow in each pipeline segment using a New Advanced Analytical Method (NAAM). The number of pipeline segments considered were five. The mean area was calculated using reduced radius of flow due to the presence of deposits in the pipeline segment multiplied by the mean radial velocity of flow calculated as 0.8 of the maximum velocity across the pipeline similar to a research by Muthu & Merugu, (2015) where the effect of overlapping constriction on flow rate was investigated. Maximum velocities were obtained from the velocity profiles drawn for each pipeline segment where the maximum velocity was found to be 10 m/s. Velocity profile was obtained by plotting radial velocity across the pipe against radial distance across the pipeline similar to a research by Muthu (2015). The required predicted flow rate is shown in Table 2.

The data in Table 2 shows a summary of the design, mean predicted and actual flow rates for the control and test pipelines belonging to an oil and gas Company in Kenya.

The Table shows loss of flow rate of about 50 m³/hr in the test pipeline and 28 m³/hr in the control pipeline. The same loss is confirmed by the actual flow rates in both the control and the test pipeline. The errors are associated with the different conditions of both pipelines. A greater error in the flow rates is observed in the pipeline with deposits and corrosion than in the new pipeline free from deposits and corrosion. Figure 6 shows a similar trend of the flow rates in the two pipelines where design, actual and predicted flow rates are compared.

3.3 Predicted Flow Efficiencies in the Test and Control Pipeline

After determining the predicted and actual flow rates in the test pipeline (in section 3.2), the corresponding flow efficiencies were estimated using the modified flow efficiency model developed in this study. Table 3 shows the predicted flow efficiencies in both the test and control pipelines for five pipeline segments representing each pipeline.

The Table shows the mean flow efficiency in the test pipeline is 13% and that in the control pipeline is 55%. The mean difference between the two flows is 42%.

3.4 Validation of the Flow Efficiency Model

Various factors such as slope and pressure, influence flow efficiency in a given pipeline. The following sections illustrate the effect of these factors. A comparison of the current and existing flow efficiency models as affected by slope and pressure in oil and gas pipelines are used to validate the flow efficiency model in this study.

3.4.1 Effect of Slope on Efficiency

Slope in which the pipeline is laid is a major factor affecting flow efficiency in oil and gas pipelines. Slope values were calculated from the latitudes and longitudes of the test pipeline.

Figure 7 illustrates how the slope of the test pipeline affects its flow efficiency. The y-axis shows the flow efficiency as a percentage while the x-axis shows the various slopes of the pipeline. An S-shaped flow efficiency curve is observed. The higher the slope, the greater the flow efficiency in the pipeline and vice versa. The effect of slope on flow efficiency is 90% accurate as indicated by the coefficient of determination, R^2 .

3.4.2 Pressure Comparisons

Figure 8 shows pressure variations along the test and control pipelines. The pressure in the test pipeline was greater than that in the control pipeline as shown in the Figure. Similar results were obtained in an experimental study on the effect of inner surface roughness on pressure drop in a small diameter pipe by Goziya et al., (2020). In both cases, the pressure drop was more in the test than control pipelines.

3.4.3 Flow Efficiency Comparisons

Figure 9 shows the comparison of the different flow efficiencies in the test pipeline. The highest flow efficiency was the design flow with 72% represented as 48% followed by the actual flow efficiency with 45% represented as 29% and the least flow efficiency as the predicted flow efficiency with 40% represented as 25%.

3.5 Application of the Flow Efficiency Mathematical Model

3.5.1 Flow Efficiency Losses due to Deposits

The direct assessment of flow efficiency losses due to deposits is preferably recommended for practical applications in the oil and gas industry. The assessment is shown in Table 4 derived from the deposit flow efficiency model obtained from regression analysis.

Flow efficiency deposit model: $E\% = -5.1935\varepsilon^2 + 57.128\varepsilon - 62.321$ with $R^2 = 0.83$.

3.5.2 Flow Efficiency Losses due to Corrosion Pits

The direct assessment of flow efficiency losses due to corrosion pits is preferably recommended for practical applications in the oil and gas industry. The assessment is shown in Table 5.

Flow efficiency corrosion model: $E\% = -0.678a + 0.765$ with $R^2 = 0.82$.

3.5.3 Optimal Pigging Frequency for the Pipeline

The direct assessment of the optimal pigging frequency based on deposits and corrosion pits is preferably recommended for practical applications in the oil and gas industry. The assessment is shown in Table 6 derived from the flow efficiency and optimal flow efficiency models obtained from regression analysis.

Optimal pigging frequency (f_o) on flow efficiency (E%) model: $E\% = -7.5893f_o^2 + 65.268f_o - 42.5$ with $R^2 = 0.80$.

3.6 Flow Efficiency Chart System

A flow efficiency chart model showing the effects of deposits and corrosion on flow efficiency in the test oil and gas pipeline was developed as shown in Figure 10. A MATLAB Function, MF is used to combine the effects of deposits and corrosion on the flow efficiency in the pipeline. The chart can also be used to predict optimal pigging frequency for a desired flow efficiency and deposits in the pipeline. The Chart was developed in MATLAB Simulink environment. The chart is composed of blocks, gains, sums, constants, and display screens as shown in the Figure. The chart is applied in conjunction with the flow efficiency deposit and corrosion mathematical models. The chart is operated in MATLAB Simulink Environment. First respective deposit heights are entered in D1 and D2. The corresponding deposit coefficients are entered in DC1 and DC2. The process is summed up in SUM 1 and the results displayed in Scope 3 or the display Screen 1. To combine the effects of both deposits and corrosion pits, a MATLAB Function (MF) is applied as shown in the figure and the results displayed in Scope 2 or the display Screen 2. The chart gives the same output as the mathematical models but the results are visual and most importantly it can be used to show the effect of more than one variable with high accuracy.

4. Discussion

Pipeline flow efficiency assessment is an important part of pipeline integrity management. Its main purpose is to assess the flow efficiency and suggest corresponding plans to improve it. Previous researchers such as Ejeh et al. (2021) have proposed various methods to improve flow efficiency. They used guide vanes in curved pipelines to improve flow efficiency. At present, there is still a lack of a systematic flow efficiency assessment technology system for oil and gas pipelines.

Aiming at the safety and reliability of oil and gas pipelines as based on the analysis of existing in-line inspection data, a mathematical model for assessing the flow efficiency in oil and gas pipelines is developed. The flow efficiency mathematical model and system are shown in Equation 4 and Figure 10 respectively. Equation 4 gives the flow efficiency based on the predicted and actual flow rates while the flow efficiency chart gives flow efficiency losses due to deposits and corrosion pits in the oil and gas pipeline as shown in Table 3.

4.1 Reduced Cross-Section Areas

The height of deposits reduced the cross-sectional area of the pipeline considerably as shown in Table 1. This is confirmed by Rostron (2018) in a review paper which established that the presence of deposits in oil and gas pipelines can result to total or partial blockage of the pipeline if suitable measures to remove the deposits are not considered.

4.2 Velocity Profiles

Considering the velocity profiles, maximum velocity in the test pipeline was 10 m/s which is half that expected in an oil and gas pipeline. The normal flow velocity in oil and gas pipelines is 20 m/s. Therefore, the test pipeline is operating at half normal velocity in the pipeline mainly due to the presence of deposits and corrosion. On the other hand, maximum velocity in the control pipeline is 100 m/s. This is 10 times more than that in the test pipeline which was largely associated with absence of deposits and corrosion in addition to the bigger diameter of 500 mm as compared to the smaller diameter of 350 mm for the test pipeline. Nevertheless, the two pipes had the same pipe material and fluid characteristics.

4.3 Reduced Flow Rates

Due to reduced cross-sectional areas, the flow rates decreased. Flow rate is given as the product of cross-sectional area and velocity of flow at any location along the pipeline. The review paper by Rostron (2018) associated the losses of flow rates to the reduced cross-sectional areas due to the presence of deposit scales and wax in the pipeline.

4.4 Model Application and Validation

The flow efficiency model is used in MATLAB Simulink where the inputs of deposit and corrosion are fed into the model. The results can be obtained as for deposits effects on flow efficiency or corrosion effects on flow efficiency or a combined effect of deposits and corrosion on flow efficiency. The model can be used to predict optimal pigging frequency by assuming an optimal flow efficiency for the pipeline as desired. The ideal current industry based optimal flow efficiency for oil and gas pipelines range from 82% to 95% as given by Farshad, (2017). The model is fast, economical and user friendly. In addition, the model can be applied in other types of pipelines. Sun et al. (2019) proposed a method of predicting hydrate formation to help improve flow efficiency in gas transmission pipelines

It was observed that the total flow efficiency determined from the mathematical model and the loss in flow efficiency due to deposits and corrosion regression models was equivalent to the design flow efficiency of the pipeline with about 3% error. This implies that the model can be used to monitor flow efficiency in oil and gas pipelines.

4.5 Model Limitations

The noise associated with in-line inspections is the main cause of biases and errors in the ILI data. In addition, the ILI equipment along with the process of inspecting the pipelines is relatively costly. The main aim of this research was to develop models that can either partially or fully replace the current in-line inspections with smart pigs. In addition, the model is limited because it can only consider 2 parameters at a time with minimum pigging frequency.

4.6 Model Results and Verification

American Society of Mechanical Engineers, ASME B31.4 is a standard recommended American Petroleum Institute, API code for pipeline transportation for liquids and slurries. ASME B31.4 defines flow efficiency as the ratio between actual flow and design flow. Application of this definition on the test pipeline resulted to a actual flow efficiency of 46.5% ($\frac{400}{860} \times 100$) where 400 is the actual flow rate, 860 is the design flow rate for the pipeline and a predicted flow efficiency of 42.33% (62-19.67) where 62% is flow efficiency in the pipeline without deposits and 19.67% is the loss in flow efficiency due to deposits in the pipeline. The resulting difference between actual flow efficiency and predicted flow efficiency is 4.17% as shown in Figure 9.

The difference can be attributed to other factors affecting flow efficiency in oil and gas pipelines. These factors include varying operating conditions, slope, third party damage, vandalism, and interfaces due to multi-product flow in the pipeline. It was observed that flow efficiency increased with increasing slope.

4. Improvements of the Oil and Gas Flow Efficiency

Current measures that are applied to enhance flow efficiency include use of a proven efficiency of epoxy flow coats (Collet and Chizat, 2015), use of liquid pipeline leak detection system (Abhulimen, 2004), use of the 'Rule of Thumb' to design optimal pigging frequencies (Wenda, 2014), use of cathodic protection systems, CPS and use of chemical inhibitors such as urotropine, thiourea, o-xylene thiourea, ruthenium, and industrial xylene thiourea. The supervisory control and data acquisition, SCADA is currently being used to assess and monitor flow rates in oil and gas pipelines with an aim of improving the flow efficiency in the pipeline. In addition, the in-line inspection, ILI system is used to monitor the internal condition of oil and gas pipelines so as to enhance flow efficiency. However, both SCADA and the in-line inspection, ILI are relatively costly and alternative solutions should be sought.

5. Conclusions

This paper presents a calculation model of the volumetric flow efficiency for multi-product transmission oil and gas pipelines with uneven or non-uniform distribution of deposits and corrosion. The calculation methods of the estimated predicted oil flow rate are presented and discussed.

Based on these predictive methods developed, the following conclusions could be made:

- The model can be used to predict flow rates in the pipeline if the flow efficiency and actual flow rates are known.
- Equally, the model can be used to predict actual flow rates in the pipeline if the volumetric flow efficiency and the predicted flow rates are known.
- It was possible to determine the optimal pigging frequency estimated from the volumetric flow efficiency. This can help to remove deposits and reduce corrosion in the pipeline which in turn helps to reduce excessive pressure drops making the pipeline more productive, profitable, efficient, and safe to operate.

Acknowledgements

The Author wishes to acknowledge the following institutions for their contributions: Kenya Pipeline Company for their data access, University of South Wales for the excellent supervision of this research and the Technical University of Kenya for the moral support.

References

- [1] American Petroleum Institute (2022) B31.4 - 2022 Pipeline Transportation Systems for Liquids and Slurries. New York, API.
- [2] Abdulmalik, Goziya.A. (2020) 'Effect of inner surface roughness on pressure drop in a small pipe'. *International Journal of Novel Research in Engineering and Science*. Vol. 7, Issue 1, pp: (1-8), Available at: www.noveltyjournals.com.
- [3] Amadi, S.A. *et al.* (2007) Analysis of corrosion induced failure in oil pipelines in the marine environment and possible control measures. *Journal of Industrial Pollution Control*. ISSN (0970-2083).
- [4] Abhulimen (2004) 'Liquid Pipeline leak detection system: model development and numerical simulation'. *Chemical Engineering Journal* 97(1):47–67.
DOI:[10.1016/S1385-8947\(03\)00098-6](https://doi.org/10.1016/S1385-8947(03)00098-6).
- [5] Chuka, E. (2016) 'Transient Model-Based Leak Detection and Localization Technique for Crude', pp. 37–48. doi:10.21276/sjeat.2016.1.2.2.
- [6] Collet P. and Chizat B. (2015) 'The proven efficiency of epoxy flow coats for the protection of gas transmission pipelines', in *Pipeline Technology Conference*.
- [7] Ejeh C., Alawwa, F., Kofi, A. and Ingrid A., (2021) 'Improving flow efficiency in curved pipes during multi-phase, immiscible fluid flow using edge-tailored guide vanes', *Experimental and Computational Multi-phase Flow Journal*, 5(1). DOI:[10.1007/s42757-021-0121-7](https://doi.org/10.1007/s42757-021-0121-7).
- [8] Faik Hamad, Faraji F., Christiano G., Santim C., Basha N., Ali Z., (2017) 'Investigation of pressure drop in horizontal pipes with different diameters, ' *International Journal of Multiphase Flow*.'
- [9] Farshad, F. (2017) 'Pipeline optimization - A surface roughness approach'.
E-mail: Farshad@louisiana.edu.
- [10] Goziya W., Adekola A. & Abdulmalik T., (2020) 'Effect of Inner Surface Roughness on Pressure Drop in a Small Diameter Pipe'. *International Journal of Research in Engineering & Pharmaceutical Sciences* 7(1): 1-8.

- [11] George P. Kouropoulos (2014) 'The Effect of the Reynolds Number of Air Flow to the Particle Collection Efficiency of a Fibrous Medium with Cylindrical Section'.
- [12] H.Alamri, A. (2020) 'Localized corrosion and mitigation approach of steel materials used in oil and gas pipelines – An overview', *Engineering Failure Analysis*.
- [13] Harrison B., Falcone G., Hewitt G., Alimenti, C. (2002) 'Multiphase Flow Metering: Current Trends and Future Developments', in *SPE Annual Technical Conference and Exhibition*.
- [14] Sun, B., (2019) 'Prediction of hydrate deposition in pipelines to improve gas transportation efficiency and safety', *Applied Energy*.
- [15] JimiaoDuana, S., Denga S., XubHuishu, L., MingChena, J. (2018) 'The effect of gas flow rate on the wax deposition in oil-gas stratified pipe flow', *Journal of Petroleum Science & Engineering*, 162, pp. 539–547.
- [16] Karina Shamilyevna Nurgalieva, L.A.S. and Masoud R. (2021) 'Improving the Efficiency of Oil and Gas Wells Complicated by the Formation of Asphalt-Resin-Paraffin Deposits', *Energies*, 14(20)Formation of Asphalt–Resin–Paraffin Deposits', *Energies*, 14(20).
- [17] Kiefner J., (2001) 'Oil pipeline characteristics and risk factors report
- [18] Lofti (2019) 'Efficiency of the Flow in the Circular Pipe'. *Journal of Urban and Environmental Engineering* 8(1), pp. 3-10.
- [19] Kamau J., (2018) 'Crisis meeting at Kenya Pipeline as fuel loss now climbs to KSh. 2.3 billion.' Daily Nation No. 19502. www.nation.co.ke.
- [20] Lu, H. Behbahani, S., & Azimi, M. Matthews, J.C., Han, S., & Iseley, T. (2020) 'Trenchless construction technologies for oil and gas pipelines: State-of-the art review'. *Journal of Construction Engineering and Management*, 146(6).
- [21] M.Askaria M.Aliofkhazraeia S.Afroukhtehb (2019) 'A comprehensive review on internal corrosion and cracking of oil and gas pipelines', *Journal of Natural Gas Science and Engineering*, 71.
- [22] MirHassan & Ghorbanalizadeh (2008) 'Batching in Multi-Product Petroleum Transmission Pipelines'. *Journal of Chemical Engineering Science. Vol 220 (2020)*.

- [23] Nikolaos A. Tsochatzidis, K. (2007) 'Methods help remove black powder from gas pipelines', *Oil & Gas Journal*, 105(10).
- [24] Ram S. (2019) 'Continuity Equation'.
- [25] Rostron, P. (2018) 'Critical Review of Pipeline Scale Measurement Technologies', *Journal of Indian Science and Technology*.
- [26] Salama Amgad (2021) 'Velocity Profile Representation for Fully Developed Turbulent Flows in Pipes: A Modified Power Law', *Fluids* 2021, 6(10),369; <https://doi.org/10.3390/fluids6100369>.
- [27] Sadaf, M. (2019) 'Interface Management during Transportation of Products through Multi-Product Petroleum Pipelines without Kerosene Plug', *Journal of The Institution of Engineers (India)*, 100(3), pp. 587–590.
- [28] Tolumoye Ajoko, Tari Kilakime, Ernest Peretiye Apresai, P. (2022) 'Mathematical Approach for Pressure Loss Determination in Oil and Gas Pipelines', *International Journal of Scientific Research in Science and Technology*, pp. 220–226.
- [29] Weimin Bao, Junwei Zhou, Xiaohua Xiang, P.J. 3 and Muxi B. 4 (2018) 'settings Open Access Article A Hydraulic Friction Model for One-Dimensional Unsteady Channel Flows with Experimental Demonstration', *Water*.
- [30] Wenda, W. (2014) 'Identifying optimal pigging frequency for oil pipelines subject to non-uniform wax deposition distribution'. <https://doi.org/10.1115/IPC2014-33064>
- [31] Wamugo M. (2011) Kenya: KPC Investigating Fire Tragedy. The Star.
- [32] Xie, Y., Cui, M. and Yuan, Z. (2015) 'A calculation model for gas transmission efficiency of long distance pipelines', *Open Fuels and Energy Science Journal*, 8(2), pp. 375–378.
- [33] Zahid Umer, Kamran Khan and Sohaib Khan (2018) 'A methodology of flexibility Analysis of pipeline systems. *Volume 233, Issue 4*.

Figures

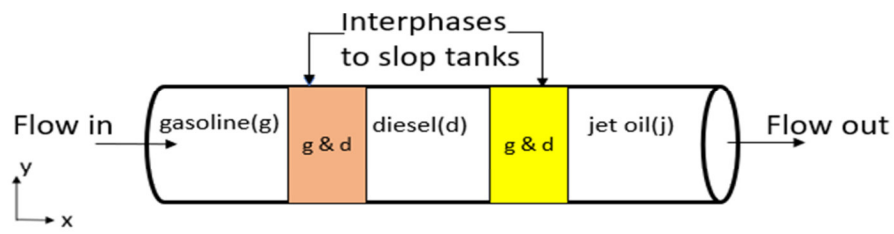


Figure 1. A typical multi-product pipeline

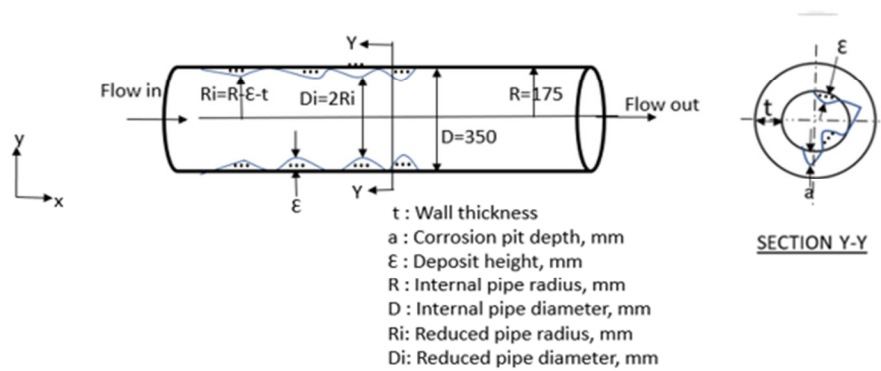


Figure 2. Deposits and corrosion non-uniformly distributed throughout the pipeline

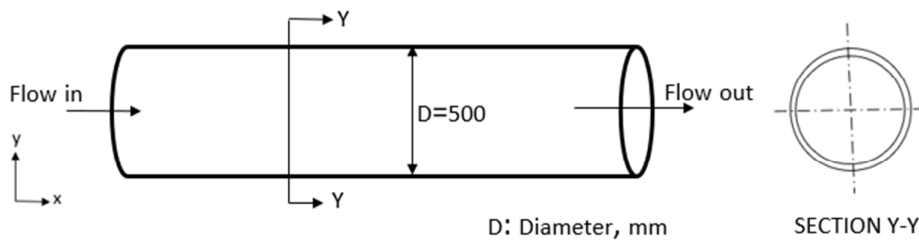


Figure 3. A new oil and gas pipeline without deposits and corrosion

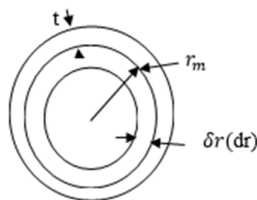


Figure 4 Area of flow through the pipeline segment

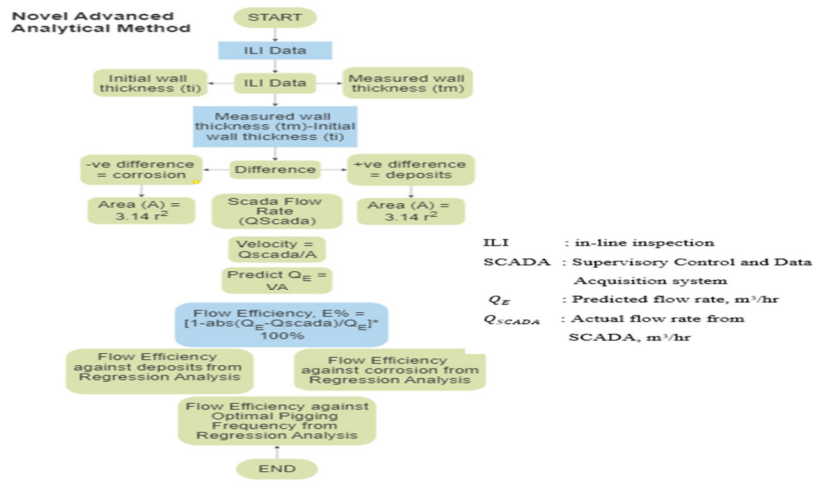


Figure 5. Estimating predicted flow rate in oil and gas pipelines

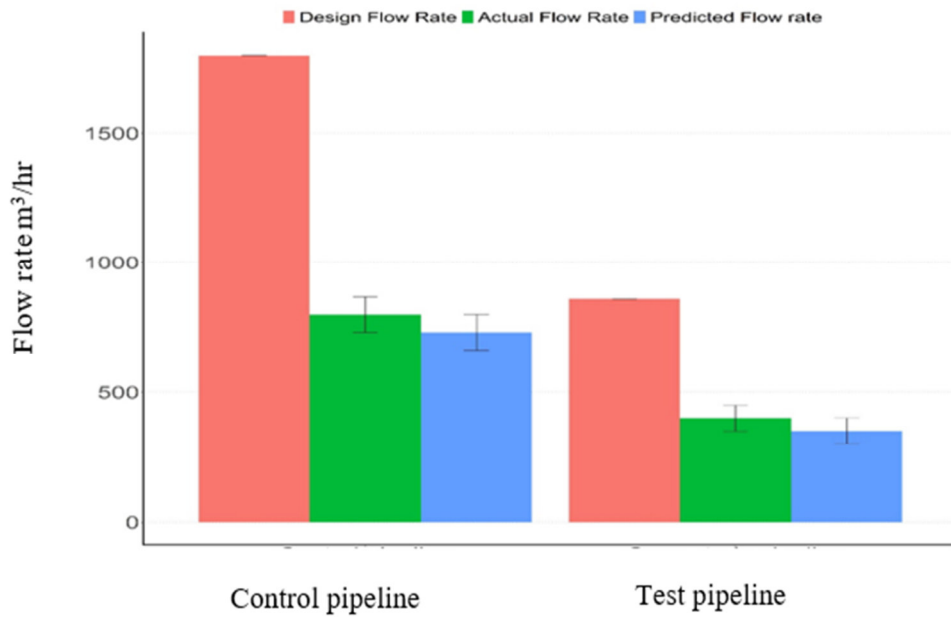


Figure 6. Trend of the flow rates in the control and test pipelines

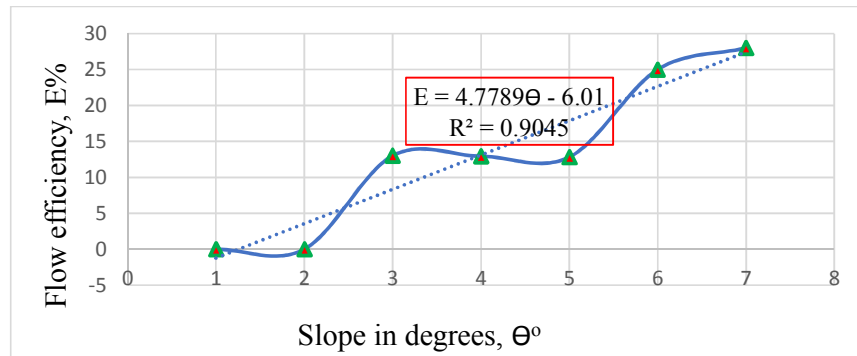


Figure 7. Effect of slope on the volumetric flow efficiency in the pipeline

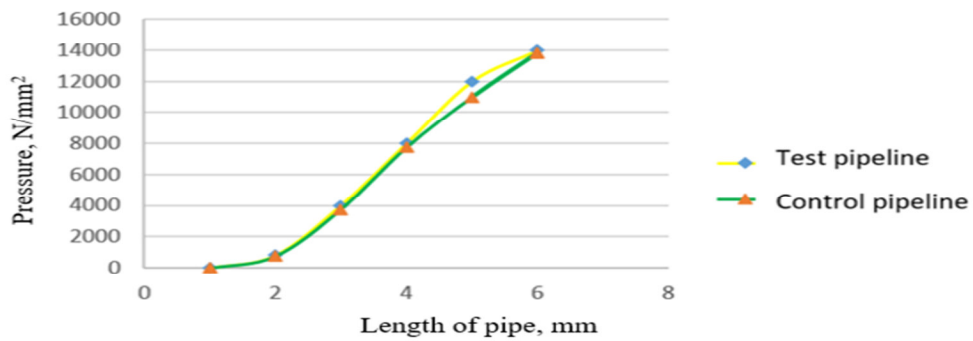


Figure 8. Relationship between pressure loss in test and control pipelines

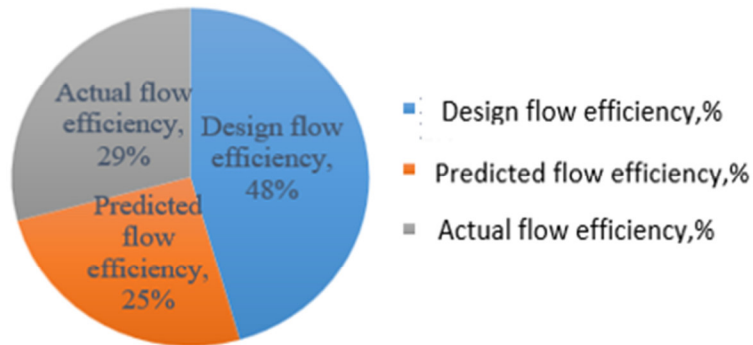


Figure 9. Flow efficiencies in the pipeline segments

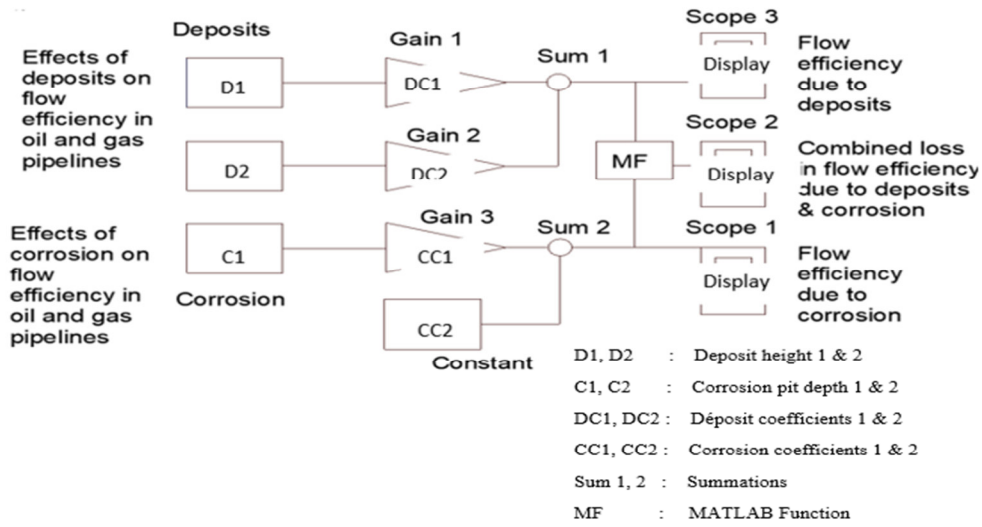


Figure 10 Flow efficiency chart model

Tables

Table 1. Actual flow rates in the test and control pipelines

Pipeline segment (No)	Actual Flow Rate in Test Pipeline (m ³ /hr)	Actual Flow Rate in Control Pipeline (m ³ /hr)
1	400	760
2	400	760
3	400	760
4	400	760
5	400	760

Table 2. Comparing flows in the control and test pipelines

	Design flow rate m ³ /hr	Predicted flow rate m ³ /hr	Actual flow rate m ³ /hr	Error m ³ /hr
Control pipeline	1800	732	760	28
Test pipeline	860	350	400	50

Table 3. Flow efficiencies in the test and control pipeline

Pipe segment	Flow efficiency in the test pipeline, E%	Flow efficiency in the control pipeline, E%
1	13	55
2	13	55
3	13	55
4	13	55
5	13	55

Table 4. Flow efficiency losses due to deposits in the test pipeline

Deposit, mm	Predicted flow efficiency losses, %	Actual flow efficiency %,
0	62.3 (Base flow efficiency)	62.3
1	10	52.3
1.2	1.12	51.1
1.3	1.19	47.9

Table 5. Shows flow efficiency losses due to corrosion pits in the test pipeline

Corrosion, a mm	Flow efficiency losses, E%
0	0
1	0.31
1.2	0.51
1.3	0.60

Table 6. Optimal pigging frequency for the pipeline

Pipeline	Recommended optimal flow efficiency, E_o %	Predicted flow efficiency, E%	Predicted optimal pigging frequency (f_o), weeks	Existing optimal pigging frequency (f_o), weeks
Test pipeline	82	13	2-3	2-3
Control pipeline	92	55	-	12